HHS Public Access

Author manuscript

Cancer Gene Ther. Author manuscript; available in PMC 2023 September 13.

Published in final edited form as:

Cancer Gene Ther. 2023 April ; 30(4): 608–621. doi:10.1038/s41417-022-00575-x.

FAP is critical for ovarian cancer cell survival by sustaining NF-κB activation through recruitment of PRKDC in lipid rafts

Bin Li[1,†], **Zuo Ding**[1,†], **Ozlem Calbay**[1], **Yue Li**[1], **Tao Li**[1], **Lingtao Jin**[2], **Shuang Huang**[1,*]

[1]Department of Anatomy and Cell Biology, University of Florida College of Medicine, Gainesville, FL 32611.

[2]Deparment of Molecular Medicine, The University of Texas Health Science Center at San Antonio, San Antonio, TX 78245.

Abstract

Fibroblast activation protein (FAP) is tumor-specific and plays an important role in tumorigenecity. However, agents against its enzymatic activity or extracellular presence were unsuccessful in the clinic for undefined reasons. Here we show that FAP expression is higher in advanced ovarian cancer and is only detected in invasive ovarian cancer cells. Silencing FAP induces apoptosis and FAP's enzymatic activity is dispensable for cell survival. To elucidate the cause of apoptosis, we find that NF-κB activity is diminished when FAP is depleted and BIRC5 (survivin) acts downstream of FAP-NF-κB axis to promote cell survival. To uncover the link between FAP and NF-κB activation, we reveal that PRKDC (DNA-PK, DNA-dependent protein kinase) forms complex with FAP and is required for NF-κB activation and cell survival. Remarkably, FAP-PRKDC interaction occurs only in lipid rafts and depleting FAP prevents lipid raft localization of PRKDC. Given the known ability of PRKDC to direct NF-κB activation, these results suggest that FAP recruits PRKDC in lipid rafts for NF-κB activation. FAP's non-enzymatic role and functioning from lipid rafts for cell survival also offer an explanation on the failure of past FAP-targeted therapies. Finally, we demonstrate that EpCAM aptamer-delivered FAP siRNA impeded intraperitoneal xenograft development of ovary tumors.

INTRODUCTION

Ovarian cancer is the deadliest gynecological cancer and high mortality rate is mainly due to the lack of symptom at early stage. In fact, stage I and II patients have 5-year survival of 90% and over 70% respectively while 5-year survival rate drops to 39% for stage III patients and dismal 17% for stage IV patients (1). Current mainstay of ovarian cancer therapy is the combination of surgery and chemotherapy. However, majority of patients will develop therapeutic resistance, suffer relapse and eventually succumb to the disease (2). Finding ways to prevent progression to late stage disease is expected to improve clinical outcome of

*Corresponding author: Shuang Huang, Department of Anatomy and Cell Biology, University of Florida College of Medicine, Gainesville, FL 32610. shuanghuang@ufl.edu.

†Equal contribution

COMFLICT OF INTERESTS

The authors declare no conflict of interest.

ovarian cancer patients, which may be facilitated by identifying molecules/pathways key for ovarian cancer progression and survival.

Fibroblast activation protein-alpha (FAP) is a member of the dipeptidyl peptidase (DPP) family and possesses both post-proline peptidase and gelatinase activities (3). While FAP is absent in most normal adult tissues, it is highly expressed in tumors, especially in tumor stroma (cancer-associated fibroblasts) (4). Experimental evidence from both *in vitro* and *in vivo* studies demonstrates that FAP promotes cancer cell growth and tumor progression (5-7), and enzymatic activity of FAP is believed to be a key contributor to its tumor-promoting function (3, 4, 8). However, there are reports indicating a non-enzymatic role of FAP in tumor cell growth. For example, proteinase-inactive FAP is able to increase breast cancer cell growth (9, 10). Because of FAP's tumor-specific expression and tumorigenic role, efforts have been exerted to develop small molecular inhibitors targeting FAP activity and agents targeting its extracellular presence (11-14). Alas, clinic trials with these agents showed minimal efficacy and the underlying reasons have not been addressed (15-17).

FAP is present in almost all ovarian cancers but not in normal ovary or benign ovarian tissues (18, 19). Although FAP expression in ovary cancer stroma is certain, its expression in ovarian cancer epithelial cells is controversial. Several studies reported the detection of FAP in ovarian cancer cell lines (20-22) and immunohistochemistry examination of epithelial ovarian cancer showed FAP protein present in more than 20% tumor epithelium (23). Especially, FAP immunostaining is more intense in malignant neoplasms than in benign neoplasms, as well as in moderately differentiated and undifferentiated ovarian carcinomas compared to well-differentiated neoplasms (24). Knockdown of FAP in ovarian cancer SK-OV3 cells decreased the tumor growth rate and, concordantly, forcing its expression promoted cell proliferation, drug resistance, invasiveness and tumor development (25, 26). FAP expression and activation were shown to occur most prevalently in ovarian cancer in a screen that included adenocarcinoma of the colon and stomach, invasive ductal carcinoma of the breast, and malignant melanoma (27). In addition, level of FAP is higher in the malignant effusion specimens and negatively associated with the overall survival rate of ovarian cancer patients (28). Collectively, these findings implicate FAP as a key player in ovarian cancer progression and development. Nonetheless, molecular mechanisms associated with FAP's tumorigenic role in ovarian cancer (and maybe other cancer types) remains elusive.

The purpose of this study is to identify promising therapeutic target in ovarian cancer. Particularly, we aim to investigate whether FAP remains as an ideal target in ovarian cancer as previous attempts using enzymatic inhibitors or monoclonal antibody were not successful. Through the analysis of The Cancer Genome Atlas (TCGA) and Clinical Proteomic Tumor Analysis Consortium (CPTAC) ovarian cancer data set, we identified FAP as a gene upregulated in advanced ovarian cancer. With established ovarian cancer cell lines, we observed that FAP was only detected in invasive (mesenchymal-like) ovarian cancer cells. When FAP-specific shRNA was introduced into ovarian cancer cells, we observed dramatic apoptosis in invasive ovarian cancer cells and the role of FAP in cell survival was independent of its enzymatic activity. By analyzing differentially expressed genes between control and FAP-knockdown cells and further reporter/biochemical assays, we

found that NF-κB activity was diminished in FAP-knockdown cells and BIRC5 (survivin) acted downstream of FAP-NF-κB axis to regulate cell survival. To uncover the link between FAP and NF-κB, we found that PRKDC (DNA-dependent protein kinase, DNA-PK) was an FAP-interacting protein and depletion of PRKDC suppressed NF-κB activation, BIRC5 abundance and cell viability. Intriguingly, FAP-PRKDC interaction only occurs in lipid raft and the presence of FAP is critical for lipid raft localization of PRKDC. Given the fact that PRKDC is able to activate NF-κB in various cell types, we propose that FAP controls cell survival by recruiting PRKDC in lipid rafts for subsequent NF-κB activation. Finally, we show that chimera of EpCAM aptamer and FAP siRNA obliterated intraperitoneal xenograft development of ovarian cancer.

RESULTS

FAP is upregulated in advanced stages of ovarian cancer and invasive ovarian cancer cells

To identify candidate genes critical for ovarian cancer progression, we generated a volcano plot using TCGA ovarian cancer dataset to identify mRNA differentially expressed between patients in early (Stage I and II) and advanced (Stage III and IV) stages (Log2 fold change > 1.5 and $P < 0.05$). A total of 24 genes were upregulated in advanced stages of patients while only one was downregulated (Fig.1A and Table S1). We focused on FAP because it is a proteinase and is regarded as targetable enzyme. To explore FAP's relevance to ovarian cancer, we analyzed TCGA dataset and found that FAP expression is higher in Stage III and IV patients than that in Stage II patients (Fig.1B). However, FAP expression is not associated with tumor grade (Fig.S1). Similar to what was observed with TCGA dataset, analysis of CPTAC dataset showed that level of FAP protein is higher in Stage III/IV patients than Stage 1/II (Fig.1C). Kaplan–Meier analyses further showed that FAP expression was inversely correlated with patient survival ($P = 5.1 \times 10^{-8}$ for overall survival and $P = 2.1 \times 10^{-8}$ for progression free survival) (Fig.1D and 1E).

With the aid of established ovarian cancer cell lines, we previously showed that mesenchymal-like, but not epithelial-like ovarian cancer cells were capable of undergoing robust intraperitoneal xenograft development (29-31). Using E-cadherin as an epithelial and vimentin as a mesenchymal marker, respectively, we observed that all mesenchymal-like lines were highly invasive while epithelial-like lines poorly invaded Matrigel (Fig.1F and 1G). Western blot analysis showed that FAP was only detected in invasive ovarian cancer cell lines (Fig.1G), indicating FAP is likely involved in tumorigenic events in mesenchymal-like ovarian cancer.

FAP controls ovarian cancer cell survival independent of its proteinase activity

To investigate how silencing FAP impact on ovarian cancer behaviors, we screened a set of 5 FAP shRNAs in HEY cells and were able to identify one that effectively depleted FAP expression (Fig.S2). Lentivirally transduction of this shRNA led to massive cell death in invasive ovarian cancer cell lines (FAP-expressing) while viability of non-invasive lines (FAP-negative) was not affected (Fig.2A). To rule out the off-target effect of shRNA and determine importance of FAP's proteinase function for cell viability, we introduced either wild-type or proteinase-inactive mutant form of FAP (FAP/S624A) into FAP-knockdown

cells. Cell viability assay (CCK8) showed that both forms of FAP similarly reversed the cell death triggered by FAP depletion (Fig.2B). These results not only confirmed the specificity of FAP knockdown effect but also suggest that proteinase activity is dispensable for FAP regulation of cell survival. This conclusion is further supported by the observation that metalloproteinase inhibitor Batimastat and dipeptidase inhibitor Talabostat either alone or together displayed little effect on the viability of HEY and OVCAR8 cells (Fig.S3). In a parallel experiment, we also investigated whether forcing FAP expression was able to promote ovarian cancer progression by lentivirally introducing FAP into epithelial-like OVCAR3 and OVCAR4 cells. We failed to detect obvious effect of ectopic FAP expression on cell morphology and proliferation (Fig.S4A and S4B). Western blotting analysis also did not indicated the occurrence of EMT in cells with forced FAP expression as there was no detectable difference in the abundance of E-cadherin between vector control and FAP-transduced cells (Fig.S4C). These results suggest that FAP alone is not sufficient to confer non-invasive ovarian cancer cells with more aggressive features although its presence is critical for the survival of invasive ovarian cancer cells.

To determine the cause of cells death observed in FAP-knockdown cells, we initially performed propidium iodine (PI) staining-based flow cytometry to assess cell cycle progression. In control HEY and OVCAR8 cells, we detected less than 1% of cells in sub-G1 (Fig.S5). In contrast, over 50% of FAP-knockdown cells were present in Sub-G1 (Fig.S5), suggesting the possibility of apoptosis because cells in Sub-G1 usually contain fragmented DNA, a hallmark of apoptosis. Subsequently, we employed Annexin V/PI staining-based flow cytometry to confirm the occurrence of apoptosis. We observed that approximately 12.7 and 11.67%, respectively, of total HEY and OVCAR8 cell population were apoptotic (Q2 + Q3) (Fig.2C). However, these percentages rose to 57.4 and 80.4 %, respectively, in FAP-depleted cells (Fig.2C). Parallel western blot analysis showed cleaved PARP and cleaved caspase-3 in FAP-knockdown cells but not in control cells (Fig.2D). Moreover, both pan-caspase inhibitor zVAD and caspase-3 inhibitor DEVD blocked FAP shRNA-led cell death (Fig.2E). Together, these results suggest that silencing FAP results in apoptosis of invasive ovarian cancer cells.

The presence of FAP is essential for NF-κB activation in ovarian cancer cells

To elucidate molecular mechanism underlying FAP regulation of cell survival, we performed RNAseq analysis using both control and FAP-knockdown OVCAR8 cells followed by Gene Sequence Enrichment Analysis (GSEA) and Ingenuity Pathway Analysis (IPA). Both analyses pointed to impaired tumor necrosis factor receptor (TNFR) signaling in FAP-knockdown cells (Fig.3A and 3B). As TNFR signaling is well established to regulate cell survival through NF-κB activation (32), we measured NF-κB activity by introducing luciferase reporter plasmid containing 5 x NF-κB binding sequences into both control and FAP-knockdown cells. We observed greater than 80% reduction in NF-κB activity in FAP-knockdown HEY and OVCAR8 cells in comparison to their respective controls (Fig.3C). Further ELISA-based NF-κB transactivation assay showed marked reduction of nuclear REL abundance in FAP-knockdown HEY and OVCAR8 cells (Fig.3D and Fig.S6A). To define the cause of decreased nuclear REL presence in FAP-knockdown cells, we detected dramatic reduction of both REL mRNA and protein in FAP-knockdown cells

(Fig.3E and 3F). Remarkably, knockdown of FAP did not alter the subcellular distribution of REL between cytoplasm and nucleus (Fig.S6B). To confirm that reduced NF-κB activity in FAP-knockdown cells was relevant to REL, we showed that silencing REL rendered similar inhibitory effect in NF-κB activity as the FAP depletion (Fig.3G). To determine whether reduced NF-κB activity is the cause of FAP knockdown-triggered cell death, we treated HEY and OVCAR8 cells with IMD0354 and TPCA-1, two well-characterized NF-κB inhibitors. CCK8 assay showed that both inhibitors effectively decreased cell viability (Fig.S7A and S7B). In addition, only silencing REL (but not RELA or RELB) was able to decrease cell viability (Fig.3H). These results suggest that FAP controls the survival of invasive ovarian cancer cells by sustaining REL-dependent NF-κB activation.

FAP-REL axis regulates the survival of ovarian cancer cells through BIRC5

NF-κB signaling regulates cell survival by maintaining the expression of various pro-survival proteins effectors (33). Hence, we compared the levels of known NF-κB-regulated pro-survival proteins between control and FAP-knockdown cells. Western blot analysis showed that knockdown of FAP selectively diminished BIRC5 expression (Fig.4A). Similarly, knockdown of REL abrogated the expression of BIRC5 in both HEY and OVCAR8 cells (Fig.4B). To functionally link the disappearance of BIRC5 to apoptosis elicited by FAP or REL knockdown, we introduced BIRC5 shRNAs into HEY and OVCAR8 cells. CCK8 assay showed that knockdown of BIRC5 reduced cell viability of both cell lines (Fig.4C). Consistently, treatment of BIRC5 inhibitor YM155 led to marked decrease in cell viability whereas the BIRC2 inhibitor Birinapant or Mcl1 inhibitor S63845 displayed much less inhibitory effect (Fig.4D). When BIRC5 was ectopically expressed in HEY and OVACR8 cells, we found that FAP or REL shRNA lost their ability to suppress cell viability (Fig.4E). These results suggest that FAP-REL signaling axis regulates ovarian cancer cell survival through sustaining BIRC5 expression.

PRKDC is required for the survival of ovarian cancer cells

To uncover the link between FAP and NF-κB activation, FAP was immunoprecipitated from OVCAR8 cells followed by mass spectrometry (MS) analysis to identify FAP interacting proteins. As would be expected, FAP had the most hits from the MS analysis (Table S2). Among other proteins with reasonable hits, we focused on PRMT5 and PRKDC (Table S2) as both have been reported to activate NF-κB (34, 35). We introduced PRMT5 or PRKDC shRNAs into HEY and OVCAR8 cells and found that knockdown of PRKDC, but not PRMT5 reduced the cell viability (Fig.5A and S8A) and NF-κB activity (Fig.5B and S8B). Western blot analysis further showed that knockdown of PRKDC abolished REL and BIRC5 expression but exhibited less effect on FAP (Fig.5C). In contrast, knockdown of PRMT5 did not affect the abundance of FAP, REL or BIRC5 in both HEY and OVCAR8 cells (Fig.S4C).

PRKDC has been reported to promote cell survival by directly phosphorylating AKT at Ser473 (36-38) and AKT signaling pathway is well characterized for its importance in NF-κB activation (39, 40). We analyzed AKT phosphorylation in control and PRKRC-knockdown HEY and OVCAR8 cells and observed that level of AKT phosphorylation (Ser473) was almost completely abolished in PRKDC-knockdown cells (Fig.5D). Similarly, silencing FAP greatly lowered the abundance of phosphorylated AKT (Fig.5E). As the

AKT inhibitor AZD5363 diminished NF-κB activity in both HEY and OVCAR8 cells (Fig.5F), these results support the notion that PRKDC is the linker between FAP and NF-κB activation in ovarian cancer cells.

To ascertain that FAP's enzymatic activity was dispensable for FAP regulation of REL/BIRC5 expression and elevated Akt activity, we lentivirally introduced either HA-tagged wild-type or FAP (FAP/S624A) mutant into HEY cells followed by further silencing endogenous FAP (Fig.S8). Western blot analysis showed that levels of REL, BIRC5 and phosphor-Akt were nearly abolished in HEY transduced with FAP shRNA (Fig.S8). However, forcing the expression of either wild-type or FAP (FAP/S624A) mutant largely restored their amount (Fig.S9). These results suggest that FAP sustains Akt activation and REL/BIRC5 expression independent of its enzymatic activity, which is consistent with the observation that FAP's enzymatic activity is not required for ovarian cancer cell survival (Fig.2B).

FAP directly interacts with PRKDC and is key for PRKDC localization in lipid rafts

To provide mechanistic basis of PRKDC in FAP regulation of NF-κB activation in ovarian cancer cells, we performed co-immunoprecipitation experiments to determine the existence of FAP-PRKDC complex using FAP or PRKDC antibody. FAP was detected in PRKDC immunoprecipitates while PRKDC was seen in FAP immunoprecipitates (Fig.6A). Subsequent confocal microscope-based immunofluorescence staining revealed the co-localization of FAP and PRKDC in both HEY and OVCAR8 cells and the interaction appeared restricted to particular areas of the inner plasma membrane (Fig.6B).

Both FAP and PRKDC were reported to be present in lipid rafts but with unknown function (41, 42). The detection of FAP-PRKDC interaction in particular area of the inner plasma membrane prompted us to investigate whether this interaction occurred in lipid rafts. We isolated lipid raft fraction from HEY and OVCAR8 cells followed by western blot analysis to detect FAP and PRKDC. As with the well characterized lipid raft marker caveolin, both FAP and PRKDC were readily seen in lipid raft isolates (Fig.6C). Subsequent confocal immunofluorescence staining with labeled cholera toxin B (CT-B), which is frequently used to visualize lipid raft (43), showed that FAP-PRKDC interaction co-localized with CT-B staining (Fig.6D). However, disruption of lipid rafts using methyl-beta-cyclodextrin (MBC), which removes cholesterol from the plama membranes (44), yielded undetectable FAP-PRKDC co-localization in both cell lines (Fig.6E). These data indicate that FAP-PRKDC interaction occurs predominantly in lipid rafts.

Lipid rafts have long been recognized as sites of cell signaling (45). We hypothesized that FAP recruits PRKDC to lipid raft to launch signaling program for NF-κB activation. To test this possibility, we analyzed whether FAP knockdown affected the presence of PRKDC in lipid rafts. Western blot of lipid raft isolates revealed that there was little or no detectable PRKDC in FAP-knockdown cells while the level of caveolin in lipid rafts was unaltered between control and FAP-knockdown cells (Fig.6F), suggesting that absence of FAP prevents the localization of PRKDC to lipid raft but does not affect formation of lipid rafts. Confocal immunofluorescence staining further showed robust co-localization of PRKDC and CT-B staining (Fig.6G), which was not detected in FAP-knockdown cells

(Fig.6G). These results support the notion that FAP recruits PRKDC to lipid rafts, leading to NF-κB activation in invasive ovarian cancer cells.

EpCAM aptamer-FAP siRNA chimera effectively suppresses intraperitoneal ovarian cancer development

Since EpCAM is highly expressed in ovarian cancer but not in other tissues in peritoneal cavity (46), we reasoned that EpCAM aptamer represented as an ideal vehicle for FAP siRNA delivery. Therefore, we designed an EpCAM aptamer-FAP siRNA chimera in which both ends contained EpCAM aptamers and the middle portion encoded an FAP siRNA or scrambled sequence (Fig.7A). When HEY and OVCAR8 cells were treated with control (scrambled sequence) or FAP siRNA-containing aptamer, we found that EpCAM aptamer-FAP siRNA chimera reduced the cell viability by approximately 80% in comparison to control (Fig.7B). To evaluate the efficacy of EpCAM aptamer-FAP siRNA chimera to impede ovary tumor development, female athymic nude mice were intraperitoneally injected with luciferase-expressing HEY or OVCAR8 cells. After 1 week of tumor cell injection, scramble control or FAP siRNA-containing aptamer was administered at 5 nmole/mouse once every other day. Weekly bioluminescence imaging showed that both HEY and OVCAR8 cells underwent effective intraperitoneal xenograft development in mice receiving control aptamer (Fig.7C and 7D). In contrast, administrating EpCAM aptamer-FAP siRNA chimera deterred tumor development (Fig.7C and Fig.7D). At 5 weeks of post-treatment, all mice were euthanized and peritoneal metastatic colonization was visualized. Tumor implants were much less frequent and smaller in size in mice receiving EpCAM aptamer-FAP siRNA chimera than those in mice administered with control aptamer (Fig.7E). To quantitate the difference, we harvested tumor implants from euthanized mice. Tumor implant weights were significantly less in mice treated with EpCAM aptamer-FAP siRNA chimera than those in control-treated ones (Fig.7F).

To link impediment of peritoneal xenograft development to diminished FAP expression and apoptosis, we performed IHC to examine the intensity of FAP, cleaved CASP3 and TUNEL staining on harvested tumors. Strong FAP but no cleaved CASP3 or TUNEL were detected in tumors excised from control aptamer-treated mice (Fig.7G). In contrast, tumors derived from FAP siRNA-containing aptamer-treated mice displayed little FAP but robust cleaved CASP3 and TUNEL staining (Fig.7G). These results provide pre-clinic evidence that EpCAM aptamer-FAP siRNA chimera can potentially be an effective therapeutic tool against mesenchymal-like (invasive) ovarian cancer.

DISCUSSION

Ovarian cancer remains as the deadliest gynecological cancer mainly due to late diagnosis. We reason that identifying molecules and pathways key for survival of advanced ovarian cancer would facilitate the development of novel and effective therapeutic strategies. Toward this aim, we analyzed TCGA ovarian cancer dataset to gain knowledge on preferentially expressed genes in late stage of ovarian cancer. This analysis revealed that there were 24 upregulated genes in late stage tumors (Stage III/IV) compared to early stage (Stage I/II) (Fig.1A). We focused on FAP because its expression is inversely correlated with

ovarian cancer patient survival (Fig.1C and 1D). Ovarian cancers with mesenchymal signature are known to have worse overall survival (47). Immunohistological analyses of both primary and metastatic ovarian carcinoma also show that mesenchymal markers are accompanied with peritoneal dissemination and poor survival of ovarian cancer patients (48, 49). Consistent with these findings, we previously found that mesenchymal-like but not epithelial-like ovarian cancer cell lines were able to undergo robust intraperitoneal tumor development (31). These studies raised the possibility that mesenchymal-like ovarian cancers resemble advanced stages of ovarian cancer. This possibility is supported by the observation that FAP was detected in mesenchymal-like ovarian cancer cell lines (Fig.1E) and expressed a significantly higher level in late stage ovarian cancer patients (Fig.1F). Moreover, our results suggest that mesenchymal-like ovarian cancer cell lines are the proper experimental tools to interrogate tumorigenic role of FAP.

FAP promotes cell proliferation and migration of various cancer types including oral squamous cell carcinoma (6), breast (9), lung (50), gastric (51) and ovarian cancer (52) though its role in cell survival is unclear. Proteinase activity of FAP has been presumed to play a key role in its tumor-promoting function because wild-type FAP, but not proteinase-inactive FAP mutant was able to promote HEK293 xenograft development (8). However, FAP has also been shown to exerts its tumorigenic role in an enzymatic activity-independent manner, For example, both wild-type and proteinase-inactive FAP were reported to equally increase rate of breast cancer cell proliferation and migration, and antagonist against FAP's enzymatic activity did not affect breast xenograft development (9). In this study, we found that the proteinase activity is dispensable for FAP's role in cell survival because proteinase-inactive FAP mutant was able to prevent FAP-knockdown-led apoptosis in an almost identical manner as the wild-type FAP (Fig.2B) and FAP enzymatic inhibitors were unable to alter cell viability (Fig.S2). Our findings offer a strong argument that the role of FAP in cell survival is independent of its enzymatic activity. It is possible, nonetheless, that FAP's enzymatic activity in cancer associated stroma can still provide accessory tumor-promotion such as extracellular matrix remodeling and growth stimulation. Importantly, non-enzymatic role of FAP in cell survival provide an explanation on the failure of proteinase-targeted FAP antagonists in the clinic.

PI3K/AKT signaling pathway has been linked to FAP's capability to promote cell proliferation and migration (6, 50). Using RNAseq analysis and NF-κB promoter/activation assays, we found that NF-κB activation was impaired in FAP-knockdown cells due to diminished REL expression (Fig.3). NF-κB signaling is regarded as the most dominant cell survival mediator mainly through regulating the expression of pro-survival genes (53). We observed that depletion of either FAP or REL abolished BIRC5 in ovarian cancer cells (Fig.4A and 4B). As forced BIRC5 expression blocked apoptosis elicited by FAP or REL knockdown (Fig.4E) and BIRC5 was the only pro-survival protein with diminished expression in FAP-knockdown cells (Fig.4A), we conclude that BIRC5 acts downstream of FAP-NF-κB axis for the survival of invasive ovarian cancer cells. BIRC5 is highly expressed in ovarian cancer (54) and its expression is associated with tumor metastasis and chemoresistance (55). A recent study showed that depletion of BIRC5 or inhibition of its function suppressed growth of both ovarian primary and metastatic tumors (56). It is worthy to point out that BIRC5 has been linked to epithelial to mesenchymal transition in

ovarian cancer cells (57). Our observation that FAP was only detected in mesenchymal-like (invasive) ovarian cancer cells (Fig.1F) supports the function linkage between FAP and BIRC5, and is consistent with the unique role of FAP in the survival of advanced ovarian cancer (mesenchymal-like).

Despite studies delving into tumorigenic role of FAP, knowledge on how FAP elicits its signal is scarce. Through MS analysis of FAP immunoprecipitates, we identified PRKDC as a critical participant in FAP-NF-κB-BIRC5 cell survival axis because knockdown of PRKDC diminished NF-κB activation and BIRC5 expression in invasive ovarian cancer cells (Fig.5A-5C). PRKDC is a direct AKT activator (37) while AKT activates NF-κB either through the IKK complex or by directly phosphorylating REL/RELA subunit (39, 40). Our study showed that silencing either FAP or PRKDC reduced AKT phosphorylation and we further showed that AKT inhibitor abrogated NF-κB activation (Fig.5D and 5E). These results imply that PRKDC is the mediator between FAP and NF-κB activation in ovarian cancer cells. In cancer-associated fibroblast, FAP is present on the cell surface to remodel extracellular matrix (58) while PRKDC localizes in the nucleus to function with the Ku70/Ku80 heterodimer protein in DNA double strand break repair and recombination (59). To our surprise, FAP-PRKDC interaction occurs only in lipid rafts of ovarian cancer cells (Fig.6A-6E). Especially, depletion of FAP abolished localization of PRKDC in lipid rafts (Fig.6F and 6G), prompting us to speculate that that FAP serves as an anchor for PRKDC recruitment to lipid rafts. Although lipid raft localization of both FAP and PRKDC were previously reported (41, 42), the significance of such localization remains completely unknown. A conundrum is that AKT is usually activated on the plasma membrane while NF-κB activation occurs in the cytoplasm. The ability of FAP to recruit PRKDC to lipid rafts helps to reconcile the puzzle. In addition, cell survival-promoting role of FAP originated from lipid rafts also provide an explanation for the futility of agents targeting extracellular presence of FAP in the clinic.

The first siRNA drug was approved by the FDA in 2018 and multiple candidate small RNA drugs are currently in clinical development or in early phase clinic trials (60). We envision that FAP siRNA may be a promising therapeutic agent against advanced ovarian cancer because its effectiveness is not associated with FAP's enzymatic activity or extracellular presence. Taking advantage of our previously developed EpCAM aptamer delivery approach (61) and the known fact that EpCAM is highly expressed in ovarian cancer but not in other tissues in peritoneal cavity (46), we achieved efficient delivery of FAP siRNA in ovary tumors evidenced by FAP suppression and robust apoptosis in tumor specimens (Fig.7A and 7G). Importantly, we demonstrated that EpCAM aptamer-FAP siRNA chimera impeded intraperitoneal tumor development (Fig.7C-7F).

Our study demonstrates a previously unrecognized role of FAP in cell survival and showcases the effectiveness of aptamer-delivered FAP siRNA to suppress ovarian cancer progression (Fig.7). Although our study was done with the established ovarian cancer cell lines that might be imperfect models of human tumors, the consistency seen in multiple cell lines and the correlation between FAP and advanced disease stages/patient survival argue against any other confounding influence derived from experimental studies. Especially, extensive studies have proven that established cancer cell lines most likely represent or

retain the genetic features critical for tumor development and hence are well-validated tools for testing potential targeted therapies (62). In summary, our study suggests that FAP is an ideal therapeutic target of advanced ovarian cancer and has laid a foundation for using EpCAM aptamer-delivered FAP siRNA in clinic.

MATERIALS AND METHODS

Cell culture, small molecular inhibitors and chemical reagents

All cell lines were obtained from ATCC (Manassas, VA) and cultured in DMEM supplemented with 10% fetal bovine serum in a humidified incubator containing 5% CO_2 at 37°C. Transfection was performed using Lipofectamine™ 3000 Transfection Reagent (Thermo Fisher Scientific, Waltham, MA) according to manufacturer's protocol. ZVAD (Cat # S7023), DEVD (Cat # S7312), YM155 (Cat # S1130), Talabostat (PT-100) (Cat # S8455), Birinapant (Cat # S7015), Batimastat (Cat # S7155), AZD5363 (Cat # S8019), and S63845 (Cat # S8383) were obtained from Selleckchem (Houston, TX). Oligonucleotids were synthesized by Integrated DNA Technologies (Coralville, IA). Methyl-beta-cyclodextrin was purchased from Thermo Fisher Scientific.

shRNA design and lentiviral delivery system

shRNAs were designed using online tool (https://biosettia.com/support/shrna-designer/). Five FAP shRNAs were chosen and oligonucleotids encoding these shRNA sequences were subcloned into PLKO.1 (Addgene). All generated lentiviral constructs were sequenced to ensure the accuracy. Reference sequence used for FAP is with accession number NM_004460. Target shRNA sequences for FAP are 1) GCATTGTCTTACGCCCTTCAA, 2) GGCATATGCGGAATTTAAT, 3) GGTTACTGATGAACGAGTA, 4) GGTGGATTCTTTGTTTCAA and 5) GCCTGTATCAGAATCTGAA. shRNAs for other genes were designed in an identical process and only effective shRNA sequences were listed below. Reference sequences used for PRMT5, RELA, RELB, REL, PRKDC and BIRC5 are with accession numbers NM_004460, NM_021975, NM_006509, NM_002908, NM_006904 and NM_001168 respectively. Target shRNA sequences for PRMT5 are 1) GCCCAGTTTGAGATGCCTTAT and 2) GCGTTTCAAGAGGGAGTTCAT. Target shRNA sequences for RELA are 1) CGGATTGAGGAGAAACGTAAA and 2) CACCATCAACTATGATGAGTT. Target shRNA sequences for RELB are 1) GCTGCGGATTTGCCGAATTAA and 2) AGCCCGTCTATGACAAGAAAT. Target shRNA sequences for REL are 1) GCAGGAATCAATCCATTCAAT and 2) CTTCAGTTGTGCAGATAACAG. Target shRNA sequences for PRKDC are 1) GCAGCCTTATTACAAAGACAT and 2) CCAGTGAAAGTCTGAATCATT. Target shRNA sequences for BIRC5 are 1) CCGCATCTCTACATTCAAGAA and 2) CCAGTGTTTCTTCTGCTTCAA.

RNA sequencing and RT-qPCR

Total RNA was extracted using RNeasy Kit (Qiagen, Germantown, MD). For RNA sequencing, RNA (2μg per sample) was sent to University of Florida Interdisciplinary Center for Biotechnology Research (UF ICBR) and sequencing was done on Illumina NovaSeq6000. Raw RNA sequencing data were processed using STAR-

htseqcount-deseq2 packages in galaxy (https://usegalaxy.org/). Generated data were analyzed using web-based GSEA (https://www.gsea-msigdb.org/gsea) and IPA (https://resources.qiagenbioinformatics.com). RNA sequencing data has been deposited in Gene Expression Omnibus (GEO) with accession number GSE201244.

RT-qPCR was performed using SYBR™ Green Master Mix (Thermo Fisher Scientific). Primer pairs used are FAP-Forward (5'-ATGAGCTTCCTCGTCCAATTCA-3'), FAP-Reverse (5'-AGACCACCAGAGAGCATATTTTG-3'); BIRC5-Forward (5'-GAGGCTGGCTTCATCCACTG-3'), BIRC5-Reverse (5'-ATGCTCCTCTATCGGGTTGTC-3'); REL-Forward (5'-GCAGAGGGGAATGCGTTTTA-G-3'), REL-Reverse (5'- AGAAGGGTATGTTCGGTTGTTG-3'); GAPDH:-Forward (5'-ACAACTTTGGTATCGTGGAAGG-3'), GAPDH-Reverse (5'-GCCATCACGCCACAGTTTC-3').

Immunoprecipitation and mass spectrometry

Samples for co-immunoprecipitation and mass spectrometry were prepared using Thermo Scientific™ Pierce™ Co-Immunoprecipitation Kit according to manufacturer's protocol. For mass spectrometry, samples were precipitated with anti-FAP polyclonal antibody (R&D systems, Cat # AF3715) and then sent to UF ICBR for analysis on TSQ Altis™ Triple Quadrupole Mass Spectrometer (Thermo Fisher Scientific). For co-immunoprecipitation, samples were either precipitated with anti-FAP polyclonal antibody or goat anti-PRKDC polyclonal antibody (Abcam, Cat # ab168854).for 2 h and further with TrueBlot™ anti-Rabbit Ig Beads or TrueBlot™ anti-sheep Ig Beads ((Rockland, Limerick, PA). After several washes, beads were boiled and subjected to western blot analysis.

Construct generation

Plasmids containing FAP and BIRC5 cDNA were obtained from Arizona State University (Cat # HsCD00040283 and Cat # HsCD00003606). These plasmids were used as templates for generating full-length FAP or BIRC5 by PCR cDNA and cDNA was then subcloned into pCDH-CMV-MCS-EF1α-Puro (System Biosciences, Palo Alto, CA). To generate FAP/S624A mutant construct, point mutagenesis was performed using Q5® Site-Directed Mutagenesis Kit (New England Biolabs, Ipswich, MA) with primer sets of Forward (5'- ATGGGGCTGGGCCTATGGAGG-3') and Reverse (5'-ATGGCTATTCTTTTTTCATCAATGAAACCCATTTC -3'). All newly generated plasmids were subjected to DNA sequence analysis to ensure the accuracy.

Western blotting

Cells were harvested using RIPA Lysis and Extraction Buffer (Thermo Fisher Scientific) supplemented with Halt™ Protease and Phosphatase Inhibitor Cocktail (Thermo Fisher Scientific). Equal amounts of protein were loaded per lane into SDS-PAGE gel followed by transferring onto a nitrocellulose membrane. Membranes were blocked with 5% nonfat dried milk followed by incubation with the respective antibodies overnight. After three washes, membranes were further incubated with appropriate secondary antibodies and imaged .using Amersham Imager 600 Series (GE Healthcare, Chicago, IL). Antibodies used for western blot analysis are FAP (R&D systems, Cat # AF3715), Apoptosis Antibody Sampler Kit

(CST, Cat # 9915), p-AKT (CST, Cat # 4060), AKT (CST, Cat # 4685), NF-κB Family Antibody Sampler Kit II (CST, Cat # 55764), GAPDH (CST, Cat # 5174), PRKDC (Abcam, Cat # ab32566), PRMT5 (Abcam, Cat # ab109451).

Cell growth, in vitro invasion, flow Cytometry-based apoptosis and lipid raft isolation

Cell growth was analyzed using CCK-8 reagents (Sigma-Aldrich, St. Louis, MO). Briefly, CCK-8 reagent was added to cells cultured in 96-well plates for 2 h at 37°C followed by measuring absorbance using a Bio-Rad plate reader at 460nm. *In vitro* invasion was assayed using Matrigel invasion chamber available from Cell Biolabs Inc (San Diego, CA) according to manufacturer's protocol. Flow cytometry-based cell apoptosis was determined using Dead Cell Apoptosis Kits with Annexin V (Thermo Fisher Scientific) according to manufacturer's protocol. Lipid raft fractions were prepared using Minute™ Plasma Membrane-Derived Lipid Raft Isolation Kit (Invent Biotechnologies, Plymouth, MN) according to manufacturer's protocol.

NF-κB promoter activity assay, NF-κB family member activation assay

NF-κB transcriptional activity was analyzed using NF-κB reporter gene construct obtained from Promega (Madison, WI). To determine NF-κB activity, this plasmid was co-transfected into cells with a Renilla luciferase gene-containing plasmid (pRL-TK, Promega) for 36 h. Cells were lysed and cell lysates were assayed for luciferase activity using Dual-Luciferase® Reporter Assay System (Promega). Renilla luciferase activity was used as an internal transfection control for standardization. Nuclear activation activity of individual NF-κB family member was analyzed using TransAM® NFκB Family kit (Active Motif, Carlsbad, CA) according to manufacturer's protocol.

Immunofluorescence staining

Cells were plated on coverslips for overnight and then fixed with 4% paraformaldehyde. After permeabilization with 1% Triton X-100, fixed cells were briefly blocked with 3% BSA, then incubated with anti-FAP mAb (Cat # sc-65398, Santa Cruz Biotechnology, Santa Cruz, CA) or anti-PRKDC polyclonal antibody (Cat # ab32566, Abcam) for 1 h and further with secondary antibody (Alexa Fluor® 488 and Alexa Fluor® 568, Thermo Fisher Scientific) for another hour. Coverslips were mounted on glass slides using ProLong™ Diamond Antifade Mountant with DAPI (Thermo Fisher Scientific) and cell fluorescence staining was viewed with confocal microscopy (Carl Zeiss Vision, LSM510). To locate lipid rafts, recombinant Cholera toxin subunit B conjugated with Alexa Fluor™ 647 (Cat # C34778, Thermo Fisher Scientific) was included during incubation with secondary antibody.

Generation of EpCAM aptamer-scramble and EpCAM aptamer-FAP siRNA chimeras

T7 promoter sequence was annealed with oligonucleotides containing either sense or antisense EpCAM aptamer-FAP siRNA chimera sequence (or scrambled sequence) and then subjected to *in vitro* transcription using RiboMAX™ Large Scale RNA Production Systems (Promega). 2'-fluoro (F)- deoxycytidine and deoxyguanosine (TriLink Biotechnologies, San Diego, CA) were included in *in vitro* transcription reaction. After reactions, sense and antisense strands were annealed to generate chimeras. The configuration of the chimera was

analyzed using Forna package (http://rna.tbi.univie.ac.at/forna/). Oligonucleotides used for *in vitro* transcription are T7 Promoter (5'-AATTTAATACGACTCACTATAG-3'), EpCAM Aptamer-FAP siRNA sense (5'-CTTTGAAGGGCGTAAGACAATGCTTACGACCGGGTAACCAGTCGCCTATAGTGAGTCGTATTAAATT-3'), EpCAM Aptamer-FAP siRNA antisense (5'-GCATTGTCTTACGCCCTTCAATTACGACCGGGTAACCAGTCGCCTATAGTGAGTCGTATTAAATT-3'), EpCAM Aptamer-Scrambled sense (5'-GGATGAACGAGGTATACGACTTTACGACCGGGTAACCAGTCGCCTATAGTGAGTCGTATTAAATT-3'), EpCAM Aptamer-Scrambled antisense (5'-CTTCATCACGTATAGTCGTCCTTACGACCGGGTAACCAGTCGCCTATAGTGAGTCGTATTAAATT-3').

Mouse xenograft models, imaging, and drug administration

HEY and OVCAR8 cells containing luciferase gene were intraperitoneally injected into 5–6-week-old nude female mice (1×10^6 cells/mouse) (Jackson Lab, Bar Harbor, ME) and intraperitoneal xenograft development was monitored weekly by measuring fluorescence in Xenogen IVIS-200 In Vivo Bioluminescence imaging system (PerkinElmer Inc, Waltham, MA). After 1 week of tumor cell injection, mice were randomized into two groups (5 per group) and intraperitoneally injected with EpCAM aptamer-scramble or EpCAM aptamer-FAP siRNA chimera once every other days (5nmole/mouse). At week 5, mice were sacrificed, and visible implants were collected from peritoneal cavities. Collected implants were weighed and aliquot of implants were also sent to UF Pathology core for immunohistochemistry staining of FAP, TUNEL and cleaved casapase-3. Animal studies and these procedures were approved by the Institution Animal Care Committee at University of Florida.

Data analysis

Patient data were retrieved from TCGA ovarian serous cystadenocarcinoma dataset containing 579 patients (TCGA_OV_gistic2thd2015–02–24). Volcano plot was generated using R software ggplot package (https://biocorecrg.github.io/CRG_RIntroduction/volcano-plots.html). Correlation between FAP mRNA expression and tumor stages or grades was analyzed using TCGA ovarian cancer dataset with the aid of Prism 8.3. Correlation between FAP protein abundance and tumor stages was analyzed using CPTAC dataset (PDC000110) with the aid of Prism 8.3. Kaplan–Meier curves were generated using http://kmplot.com. All experiments were performed in triplicates. Results of each experiment were reported as the means of experimental replicates. All statistical analyses were performed using PRISM 8.3 with unpaired *t* test (two-tailed). Error bars represent the standard deviation. For all tests, $P < 0.05$ was considered statistically significant.

Supplementary Material

Refer to Web version on PubMed Central for supplementary material.

ACKNOLEDGEMENTS

This is part of doctoral work of Bin Li at University of Florida College of Medicine. This work was supported by funding from NIH CA222467 (SH) and CA256482 (SH/LJ).

DATA AVAILABILITY STATEMENTS

All data generated or analysed during this study are included in this published article [and its supplementary information files].

RFERENCES

1. Society AC. Cancer Facts & Figures 2019. Atlanta, GA: American Cancer Society; 2019.
2. Chandra A, Pius C, Nabeel M, Nair M, Vishwanatha JK, Ahmad S, et al. Ovarian cancer: Current status and strategies for improving therapeutic outcomes. Cancer Med. 2019;8(16):7018–31. [PubMed: 31560828]
3. Pure E, Blomberg R. Pro-tumorigenic roles of fibroblast activation protein in cancer: back to the basics. Oncogene. 2018;37(32):4343–57. [PubMed: 29720723]
4. Fitzgerald AA, Weiner LM. The role of fibroblast activation protein in health and malignancy. Cancer metastasis reviews. 2020;39(3):783–803. [PubMed: 32601975]
5. Lo A, Li CP, Buza EL, Blomberg R, Govindaraju P, Avery D, et al. Fibroblast activation protein augments progression and metastasis of pancreatic ductal adenocarcinoma. JCI Insight. 2017;2(19).
6. Wang H, Wu Q, Liu Z, Luo X, Fan Y, Liu Y, et al. Downregulation of FAP suppresses cell proliferation and metastasis through PTEN/PI3K/AKT and Ras-ERK signaling in oral squamous cell carcinoma. Cell Death Dis. 2014;5:e1155. [PubMed: 24722280]
7. Qi M, Fan S, Huang M, Pan J, Li Y, Miao Q, et al. Targeting FAPalpha-expressing hepatic stellate cells overcomes resistance to antiangiogenics in colorectal cancer liver metastasis models. J Clin Invest. 2022;132(19).
8. Cheng JD, Valianou M, Canutescu AA, Jaffe EK, Lee HO, Wang H, et al. Abrogation of fibroblast activation protein enzymatic activity attenuates tumor growth. Mol Cancer Ther. 2005;4(3):351–60. [PubMed: 15767544]
9. Huang Y, Simms AE, Mazur A, Wang S, Leon NR, Jones B, et al. Fibroblast activation protein-alpha promotes tumor growth and invasion of breast cancer cells through non-enzymatic functions. Clin Exp Metastasis. 2011;28(6):567–79. [PubMed: 21604185]
10. Lv B, Xie F, Zhao P, Ma X, Jiang WG, Yu J, et al. Promotion of Cellular Growth and Motility Is Independent of Enzymatic Activity of Fibroblast Activation Protein-alpha. Cancer Genomics Proteomics. 2016;13(3):201–8. [PubMed: 27107062]
11. Song P, Pan Q, Sun Z, Zou L, Yang L. Fibroblast activation protein alpha: Comprehensive detection methods for drug target and tumor marker. Chem Biol Interact. 2022;354:109830. [PubMed: 35104486]
12. Xin L, Gao J, Zheng Z, Chen Y, Lv S, Zhao Z, et al. Fibroblast Activation Protein-alpha as a Target in the Bench-to-Bedside Diagnosis and Treatment of Tumors: A Narrative Review. Frontiers in oncology. 2021;11:648187. [PubMed: 34490078]
13. Simkova A, Busek P, Sedo A, Konvalinka J. Molecular recognition of fibroblast activation protein for diagnostic and therapeutic applications. Biochim Biophys Acta Proteins Proteom. 2020;1868(7):140409. [PubMed: 32171757]
14. Lee IK, Noguera-Ortega E, Xiao Z, Todd L, Scholler J, Song D, et al. Monitoring Therapeutic Response to Anti-Fibroblast Activation Protein (FAP) CAR T Cells using [18F]AlF-FAPI-74. Clinical cancer research : an official journal of the American Association for Cancer Research. 2022.
15. Narra K, Mullins SR, Lee HO, Strzemkowski-Brun B, Magalong K, Christiansen VJ, et al. Phase II trial of single agent Val-boroPro (Talabostat) inhibiting Fibroblast Activation Protein in patients with metastatic colorectal cancer. Cancer Biol Ther. 2007;6(11):1691–9. [PubMed: 18032930]

16. Eager RM, Cunningham CC, Senzer NN, Stephenson J Jr., Anthony SP, O'Day SJ, et al. Phase II assessment of talabostat and cisplatin in second-line stage IV melanoma. BMC cancer. 2009;9:263. [PubMed: 19643020]
17. Hofheinz RD, al-Batran SE, Hartmann F, Hartung G, Jager D, Renner C, et al. Stromal antigen targeting by a humanised monoclonal antibody: an early phase II trial of sibrotuzumab in patients with metastatic colorectal cancer. Onkologie. 2003;26(1):44–8. [PubMed: 12624517]
18. Garin-Chesa P, Old LJ, Rettig WJ. Cell surface glycoprotein of reactive stromal fibroblasts as a potential antibody target in human epithelial cancers. Proceedings of the National Academy of Sciences of the United States of America. 1990;87(18):7235–9. [PubMed: 2402505]
19. Zhang MJ, Yu SY, Chu BQ, Dai W. [A statistical analysis and perspective of headache-related papers covered in 2011 PubMed]. Zhonghua Nei Ke Za Zhi. 2013;52(1):34–7. [PubMed: 23710813]
20. Wilson CH, Abbott CA. Expression profiling of dipeptidyl peptidase 8 and 9 in breast and ovarian carcinoma cell lines. Int J Oncol. 2012;41(3):919–32. [PubMed: 22736146]
21. Kennedy A, Dong H, Chen D, Chen WT. Elevation of seprase expression and promotion of an invasive phenotype by collagenous matrices in ovarian tumor cells. International journal of cancer. 2009;124(1):27–35. [PubMed: 18823010]
22. Chen H, Yang WW, Wen QT, Xu L, Chen M. TGF-beta induces fibroblast activation protein expression; fibroblast activation protein expression increases the proliferation, adhesion, and migration of HO-8910PM [corrected]. Exp Mol Pathol. 2009;87(3):189–94. [PubMed: 19747910]
23. Mhawech-Fauceglia P, Yan L, Sharifian M, Ren X, Liu S, Kim G, et al. Stromal Expression of Fibroblast Activation Protein Alpha (FAP) Predicts Platinum Resistance and Shorter Recurrence in patients with Epithelial Ovarian Cancer. Cancer Microenviron. 2015;8(1):23–31. [PubMed: 25331442]
24. da Silva AC, Jammal MP, Etchebehere RM, Murta EFC, Nomelini RS. Role of Alpha-Smooth Muscle Actin and Fibroblast Activation Protein Alpha in Ovarian Neoplasms. Gynecol Obstet Invest. 2018;83(4):381–7. [PubMed: 29621774]
25. Lai D, Ma L, Wang F. Fibroblast activation protein regulates tumor-associated fibroblasts and epithelial ovarian cancer cells. Int J Oncol. 2012;41(2):541–50. [PubMed: 22614695]
26. Yang L, Ma L, Lai D. Over-expression of fibroblast activation protein alpha increases tumor growth in xenografts of ovarian cancer cells. Acta Biochim Biophys Sin (Shanghai). 2013;45(11):928–37. [PubMed: 24028972]
27. Chen D, Kennedy A, Wang JY, Zeng W, Zhao Q, Pearl M, et al. Activation of EDTA-resistant gelatinases in malignant human tumors. Cancer research. 2006;66(20):9977–85. [PubMed: 17047060]
28. Zhang MZ, Qiao YH, Nesland JM, Trope C, Kennedy A, Chen WT, et al. Expression of seprase in effusions from patients with epithelial ovarian carcinoma. Chin Med J (Engl). 2007;120(8):663–8. [PubMed: 17517181]
29. Chen H, Wu X, Pan ZK, Huang S. Integrity of SOS1/EPS8/ABI1 tri-complex determines ovarian cancer metastasis. Cancer research. 2010;70(23):9979–90. [PubMed: 21118970]
30. Yang L, Fang D, Chen H, Lu Y, Dong Z, Ding HF, et al. Cyclin-dependent kinase 2 is an ideal target for ovary tumors with elevated cyclin E1 expression. Oncotarget. 2015;6(25):20801–12. [PubMed: 26204491]
31. Fang D, Chen H, Zhu JY, Wang W, Teng Y, Ding HF, et al. Epithelial-mesenchymal transition of ovarian cancer cells is sustained by Rac1 through simultaneous activation of MEK1/2 and Src signaling pathways. Oncogene. 2017;36(11):1546–58. [PubMed: 27617576]
32. Brenner D, Blaser H, Mak TW. Regulation of tumour necrosis factor signalling: live or let die. Nat Rev Immunol. 2015;15(6):362–74. [PubMed: 26008591]
33. LaCasse EC, Baird S, Korneluk RG, MacKenzie AE. The inhibitors of apoptosis (IAPs) and their emerging role in cancer. Oncogene. 1998;17(25):3247–59. [PubMed: 9916987]
34. Wei H, Wang B, Miyagi M, She Y, Gopalan B, Huang DB, et al. PRMT5 dimethylates R30 of the p65 subunit to activate NF-kappaB. Proceedings of the National Academy of Sciences of the United States of America. 2013;110(33):13516–21. [PubMed: 23904475]

35. Basu S, Rosenzweig KR, Youmell M, Price BD. The DNA-dependent protein kinase participates in the activation of NF kappa B following DNA damage. Biochemical and biophysical research communications. 1998;247(1):79–83. [PubMed: 9636658]
36. Lu D, Huang J, Basu A. Protein kinase Cepsilon activates protein kinase B/Akt via DNA-PK to protect against tumor necrosis factor-alpha-induced cell death. The Journal of biological chemistry. 2006;281(32):22799–807. [PubMed: 16785234]
37. Bozulic L, Surucu B, Hynx D, Hemmings BA. PKBalpha/Akt1 acts downstream of DNA-PK in the DNA double-strand break response and promotes survival. Mol Cell. 2008;30(2):203–13. [PubMed: 18439899]
38. Feng J, Park J, Cron P, Hess D, Hemmings BA. Identification of a PKB/Akt hydrophobic motif Ser-473 kinase as DNA-dependent protein kinase. The Journal of biological chemistry. 2004;279(39):41189–96. [PubMed: 15262962]
39. Ozes ON, Mayo LD, Gustin JA, Pfeffer SR, Pfeffer LM, Donner DB. NF-kappaB activation by tumour necrosis factor requires the Akt serine-threonine kinase. Nature. 1999;401(6748):82–5. [PubMed: 10485710]
40. Madrid LV, Mayo MW, Reuther JY, Baldwin AS, Jr. Akt stimulates the transactivation potential of the RelA/p65 Subunit of NF-kappa B through utilization of the Ikappa B kinase and activation of the mitogen-activated protein kinase p38. The Journal of biological chemistry. 2001;276(22):18934–40. [PubMed: 11259436]
41. Lucero H, Gae D, Taccioli GE. Novel localization of the DNA-PK complex in lipid rafts: a putative role in the signal transduction pathway of the ionizing radiation response. The Journal of biological chemistry. 2003;278(24):22136–43. [PubMed: 12672807]
42. Knopf JD, Tholen S, Koczorowska MM, De Wever O, Biniossek ML, Schilling O. The stromal cell-surface protease fibroblast activation protein-alpha localizes to lipid rafts and is recruited to invadopodia. Biochim Biophys Acta. 2015;1853(10 Pt A):2515–25. [PubMed: 26209915]
43. Day CA, Kenworthy AK. Functions of cholera toxin B-subunit as a raft cross-linker. Essays Biochem. 2015;57:135–45. [PubMed: 25658350]
44. Xing Y, Gu Y, Xu LC, Siedlecki CA, Donahue HJ, You J. Effects of membrane cholesterol depletion and GPI-anchored protein reduction on osteoblastic mechanotransduction. Journal of cellular physiology. 2011;226(9):2350–9. [PubMed: 21660958]
45. Alves ACS, Dias RA, Kagami LP, das Neves GM, Torres FC, Eifler-Lima VL, et al. Beyond the "Lock and Key" Paradigm: Targeting Lipid Rafts to Induce the Selective Apoptosis of Cancer Cells. Curr Med Chem. 2018;25(18):2082–104. [PubMed: 29332565]
46. Reichert JM, Valge-Archer VE. Development trends for monoclonal antibody cancer therapeutics. Nature reviews Drug discovery. 2007;6(5):349–56. [PubMed: 17431406]
47. Cancer Genome Atlas Research N. Integrated genomic analyses of ovarian carcinoma. Nature. 2011;474(7353):609–15. [PubMed: 21720365]
48. Davidson B, Holth A, Hellesylt E, Tan TZ, Huang RY, Trope C, et al. The clinical role of epithelial-mesenchymal transition and stem cell markers in advanced-stage ovarian serous carcinoma effusions. Human pathology. 2015;46(1):1–8. [PubMed: 25455994]
49. Takai M, Terai Y, Kawaguchi H, Ashihara K, Fujiwara S, Tanaka T, et al. The EMT (epithelial-mesenchymal-transition)-related protein expression indicates the metastatic status and prognosis in patients with ovarian cancer. Journal of ovarian research. 2014;7:76. [PubMed: 25296567]
50. Jia J, Martin TA, Ye L, Meng L, Xia N, Jiang WG, et al. Fibroblast activation protein-alpha promotes the growth and migration of lung cancer cells via the PI3K and sonic hedgehog pathways. International journal of molecular medicine. 2018;41(1):275–83. [PubMed: 29115573]
51. Wang RF, Zhang LH, Shan LH, Sun WG, Chai CC, Wu HM, et al. Effects of the fibroblast activation protein on the invasion and migration of gastric cancer. Exp Mol Pathol. 2013;95(3):350–56. [PubMed: 24422232]
52. Yang W, Han W, Ye S, Liu D, Wu J, Liu H, et al. Fibroblast activation protein-alpha promotes ovarian cancer cell proliferation and invasion via extracellular and intracellular signaling mechanisms. Exp Mol Pathol. 2013;95(1):105–10. [PubMed: 23778090]
53. Hunter AM, LaCasse EC, Korneluk RG. The inhibitors of apoptosis (IAPs) as cancer targets. Apoptosis. 2007;12(9):1543–68. [PubMed: 17573556]

54. Liguang Z, Peishu L, Hongluan M, Hong J, Rong W, Wachtel MS, et al. Survivin expression in ovarian cancer. Exp Oncol. 2007;29(2):121–5. [PubMed: 17704744]

55. Chen L, Liang L, Yan X, Liu N, Gong L, Pan S, et al. Survivin status affects prognosis and chemosensitivity in epithelial ovarian cancer. International journal of gynecological cancer : official journal of the International Gynecological Cancer Society. 2013;23(2):256–63. [PubMed: 23358177]

56. Zhao G, Wang Q, Wu Z, Tian X, Yan H, Wang B, et al. Ovarian Primary and Metastatic Tumors Suppressed by Survivin Knockout or a Novel Survivin Inhibitor. Mol Cancer Ther. 2019;18(12):2233–45. [PubMed: 31515295]

57. Zhao G, Wang Q, Gu Q, Qiang W, Wei JJ, Dong P, et al. Lentiviral CRISPR/Cas9 nickase vector mediated BIRC5 editing inhibits epithelial to mesenchymal transition in ovarian cancer cells. Oncotarget. 2017;8(55):94666–80. [PubMed: 29212257]

58. Scanlan MJ, Raj BK, Calvo B, Garin-Chesa P, Sanz-Moncasi MP, Healey JH, et al. Molecular cloning of fibroblast activation protein alpha, a member of the serine protease family selectively expressed in stromal fibroblasts of epithelial cancers. Proceedings of the National Academy of Sciences of the United States of America. 1994;91(12):5657–61. [PubMed: 7911242]

59. Falck J, Coates J, Jackson SP. Conserved modes of recruitment of ATM, ATR and DNA-PKcs to sites of DNA damage. Nature. 2005;434(7033):605–11. [PubMed: 15758953]

60. Hanna J, Hossain GS, Kocerha J. The Potential for microRNA Therapeutics and Clinical Research. Front Genet. 2019;10:478. [PubMed: 31156715]

61. Rehmani H, Li Y, Li T, Padia R, Calbay O, Jin L, et al. Addiction to protein kinase Ci due to PRKCI gene amplification can be exploited for an aptamer-based targeted therapy in ovarian cancer. Signal Transduct Target Ther. 2020;5(1):140. [PubMed: 32820156]

62. Hernandez L, Kim MK, Lyle LT, Bunch KP, House CD, Ning F, et al. Characterization of ovarian cancer cell lines as in vivo models for preclinical studies. Gynecologic oncology. 2016;142(2):332–40. [PubMed: 27235858]

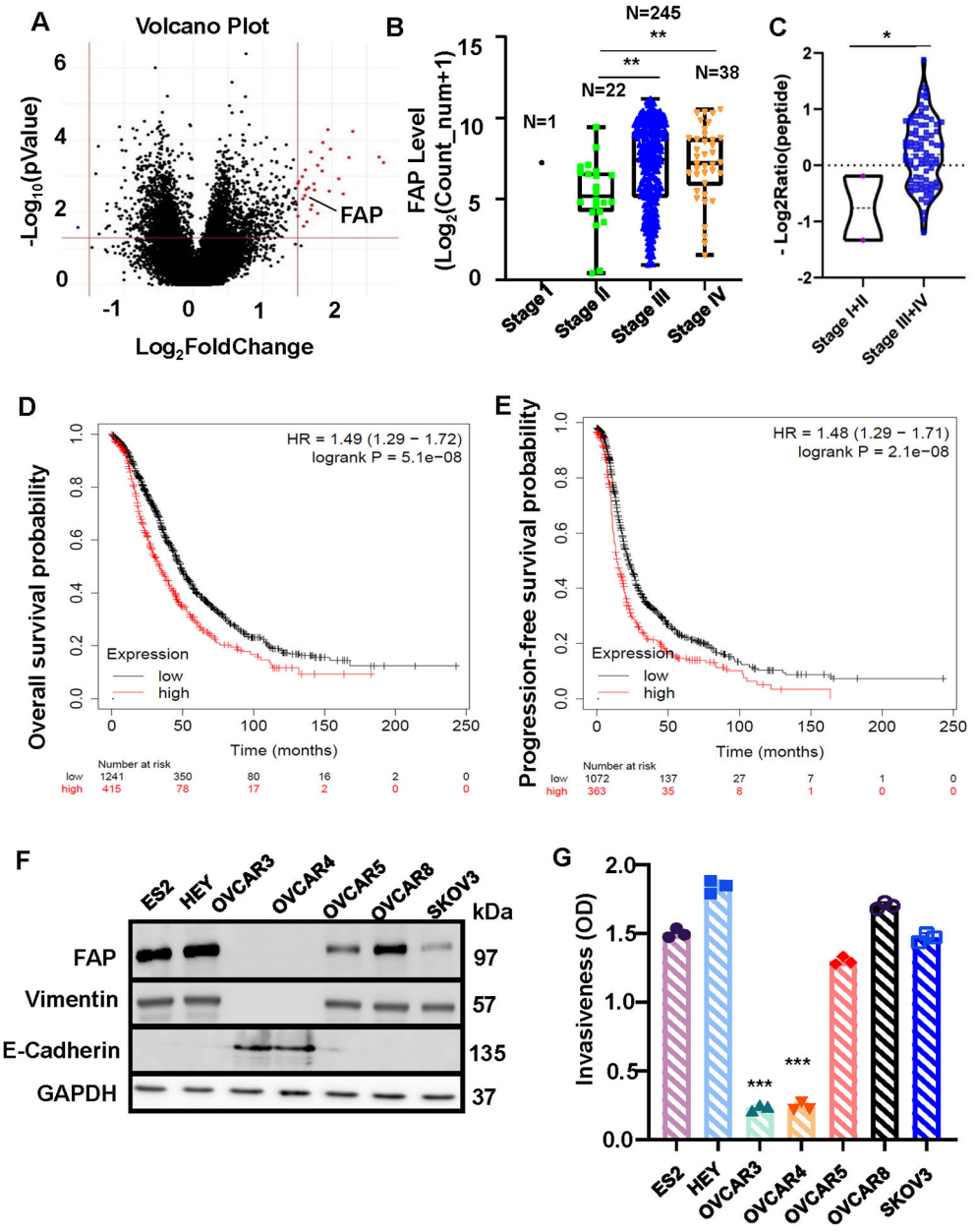

Figure 1. Higher FAP expression is associated with advanced ovarian cancer

A. Volcano plot to identify genes differentially expressed in advanced stage of ovarian cancer (Stage III/IV *vs* I/II). ***B.*** Level of FAP mRNA in Stage I, II, III and IV ovarian cancer patients. N, number of patients. **, $P < 0.01$. ***C***. Level of FAP protein in Stage 1/II and Stage III/IV. *, $P < 0.05$. ***D***. Kaplan-Meier overall survival plots of FAP. ***E.*** Kaplan-Meier progression-free survival plot of FAP. ***F***. Overnight-cultured cells were harvested for western blotting to detect FAP, vimentin, E-cadherin and GAPDH with the respective antibodies. ***G.*** Overnight-cultured cells were plated into Matrigel invasion chambers and allowed to invade for 24 h. Cells on undersurface of invasion chambers were stained while cells remaining in the chambers were removed. Stained cells were solubilized and measured using a plate reader. Data are means ± SD.

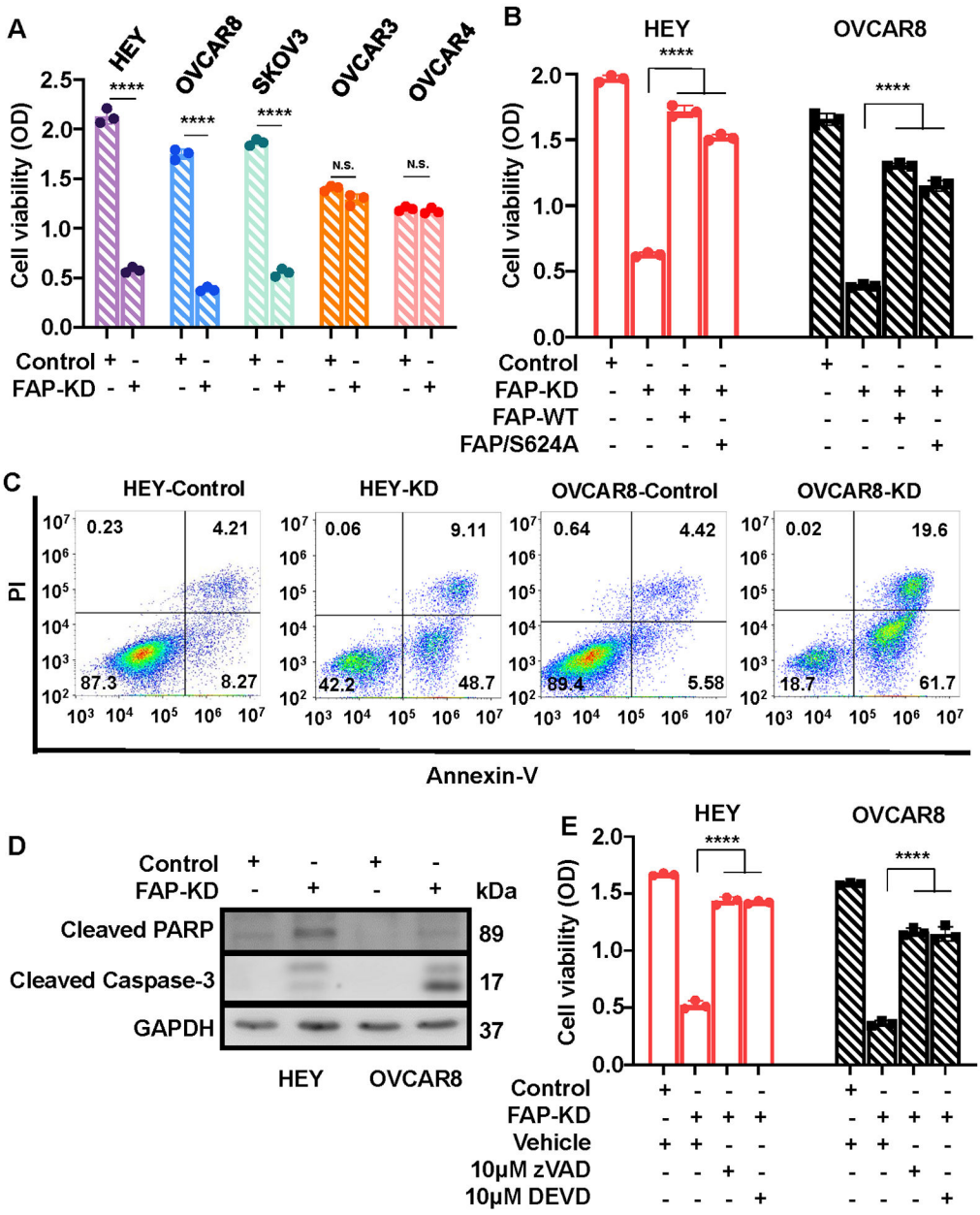

Figure 2. Knockdown of FAP leads to apoptosis of invasive ovarian cancer cells

A. Cells were lentivirally transduced with either scrambled sequence (control) or FAP shRNA for 4 days followed by CCK-8 assay to determine cell viability. Data are means ± SD. ****, $P < 0.0001$; n.s., no significance. ***B.*** HEY and OVCAR8 cells were first lentivirally transduced with FAP or FAP/S624 for 1 day and further transduced with control or FAP shRNA for additional 4 days. Cell viability was assessed by CCK-8 assay. Data are mean ± SD. ****, $P < 0.0001$. ***C***. HEY and OVCAR8 cells were lentivirally transduced with control or FAP shRNA for 4 days followed by Annexin V/PI-based flow cytometry. The horizontal axis is Annexin V staining and the vertical axis is PI staining. Cells in Quadrant 2 and 3 represent apoptotic cells. Results are representative of three independent experiments. ***D***. HEY and OVCAR8 cells were infected with lentiviral vector containing Scrambled

sequence or FAP shRNA for 4 days followed by western blotting to detect cleaved PARP, cleaved caspase-3 and GAPDH with the respective antibodies. ***E***. HEY and OVCAR8 cells were transduced with lentivirus containing scrambled sequence or FAP shRNA. One day post-infection, vehicle (DMSO), 10μM zVAD or 10μM DEVD were added to cells for additional 3 days followed by CCK-8 assay to assess cell viability. Data are means ± SD. ****, $P < 0.0001$.

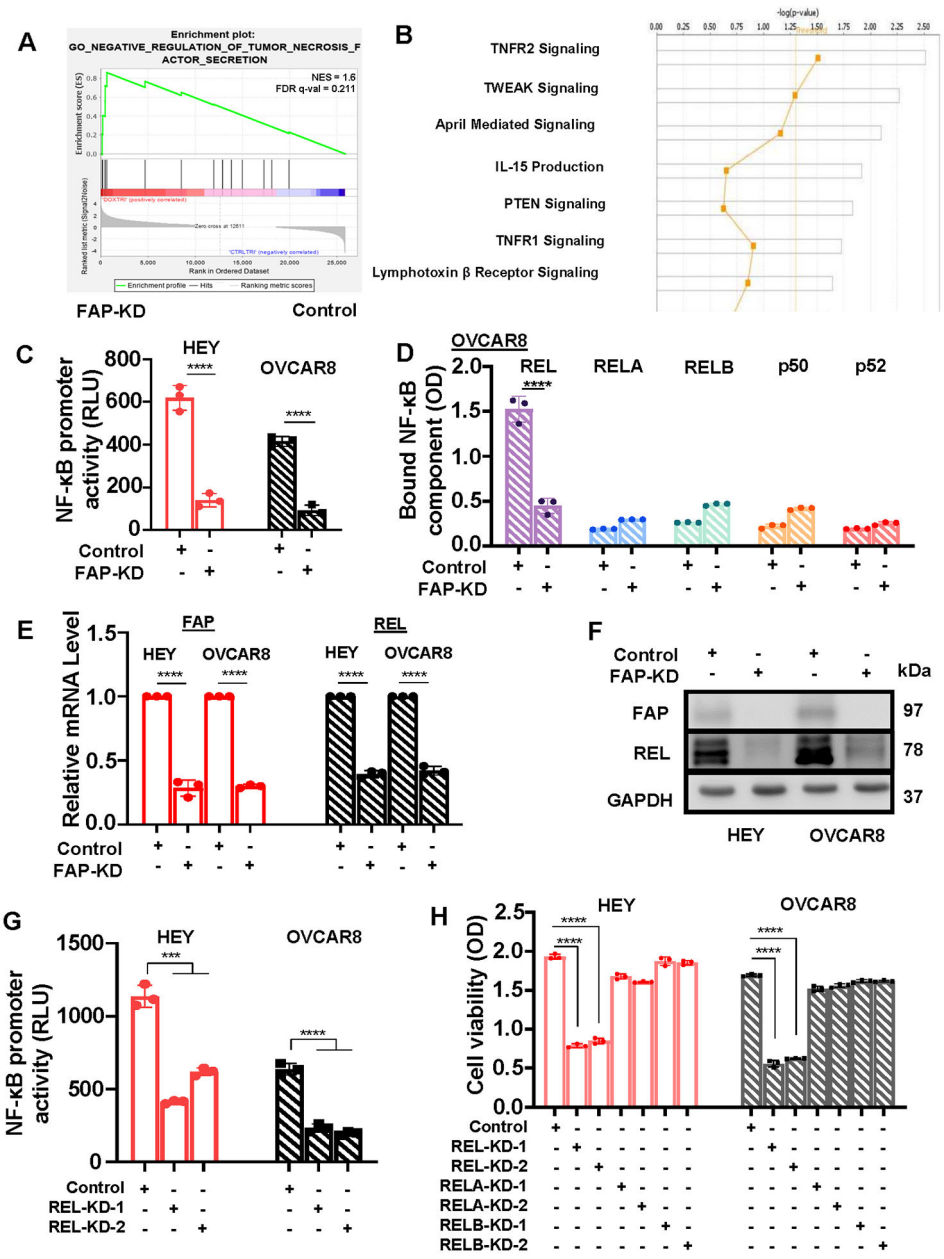

Figure 3. NF-κB signaling is impaired in ovarian cancer cells with FAP-knockdown

A, B. Total RNA was isolated from OVCAR8 cells lentivirally transduced with scrambled sequence (control) or FAP shRNA and subjected RNA sequencing. Data were analyzed by web-based Gene Sequence Enrichment Analysis (***A***) and Ingenuity Pathway Analysis (*B*). ***C***. HEY and OVCAR8 cells were lentivirally transduced with control or FAP shRNA for 2 days and then transfected with NF-κB promoter reporter construct for another day followed by measuring luciferase activity. Data are mean ± SD. ****, $P < 0.0001$. ***D***. ELISA to measure the amount of individual NF-κB family member in nuclei of OVCAR8 cells lentivirally transduced with control or FAP shRNA. Data are means ± SD. ****, $P < 0.0001$. ***E***. HEY and OVCAR8 cells were lentivirally transduced with control or FAP shRNA for 2 days followed by total RNA extraction. RNA was subjected to RT-qPCR to measure the levels of

FAP and REL mRNA using specific primer sets. GAPDH mRNA was used as an internal control for standardization. Data are means ± SD. ****, $P < 0.0001$. ***F***. Western blot analysis to detect FAP, REL and GAPDH in HEY and OVCAR8 cells transduced with control or FAP shRNA. ***G***. HEY and OVCAR8 cells were lentivirally transduced with control or REL shRNA for 2 days and then transfected with NF-κB promoter reporter construct for another day followed by measuring luciferase activity. Data are mean ± SD. ****, $P < 0.0001$. ***H***. HEY and OVCAR8 cells were lentivirally transduced with control, REL, RELA or RELB shRNA for 4 days followed by CCK-8 assay to assess cell viability. Data are mean ± SD. ****, $P < 0.0001$.

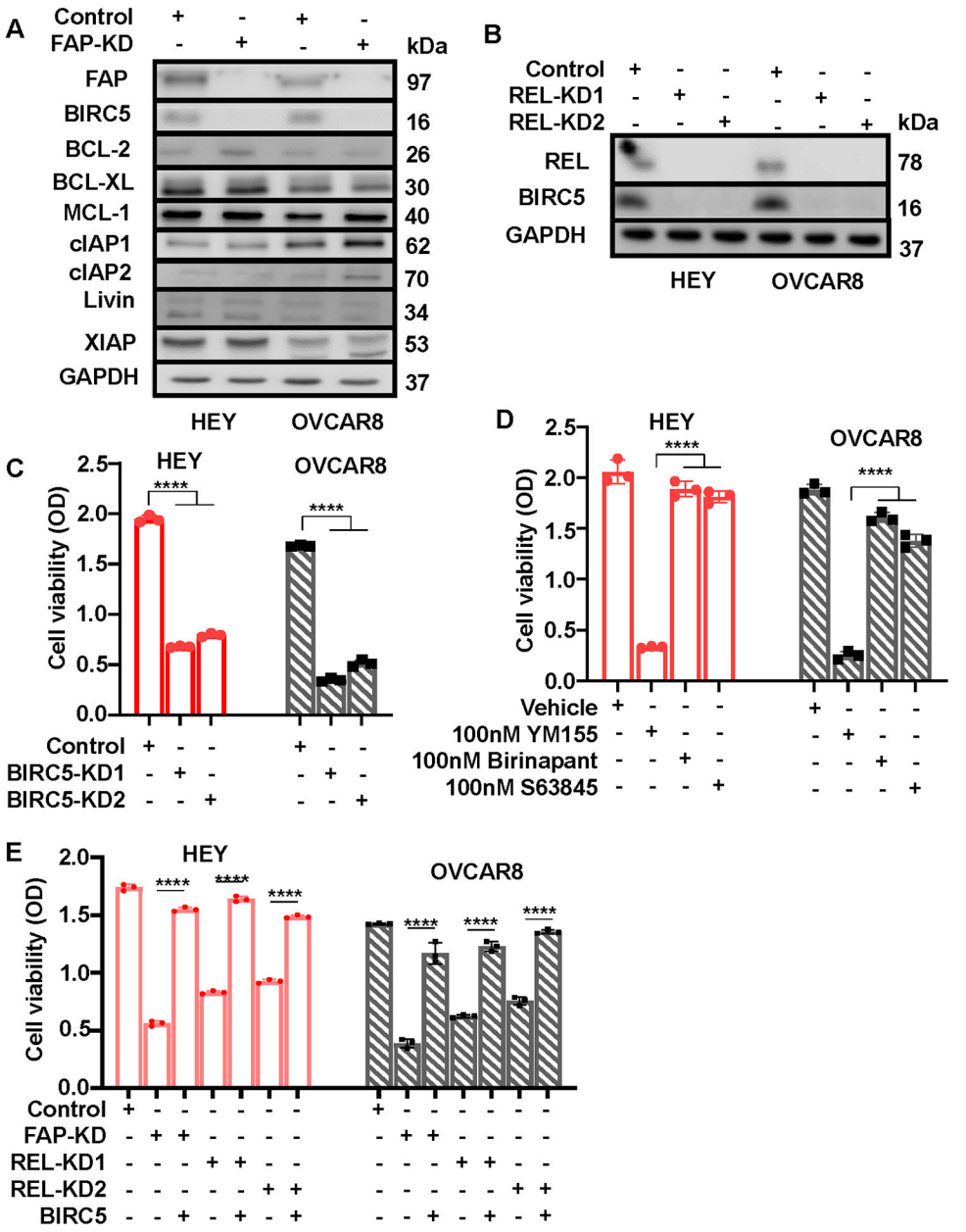

Figure 4. BIRC5 is downstream of FAP-NF-κB axis regulating ovarian cancer cell survival

A. HEY and OVCAR8 cells were lentivirally transduced with control or FAP shRNA for 3 days and then lysed for western blotting to detect FAP and a panel of pro-survival proteins with the respective antibodies. ***B***. HEY and OVCAR8 cells were lentivirally transduced with control or REL shRNA for 3 days and then lysed for western blotting to detect REL, BIRC5 and GAPDH. ***C***. HEY and OVCAR8 cells were lentivirally transduced with control or BIRC5 shRNA for 4 days followed by CCK-8 assay to assess cell viability. Data are mean ± SD. ****, $P < 0.0001$. ***D***. HEY and OVCAR8 cells were treated with vehicle (DMSO), 100nM YM155, 100nM Birinapant or 100nM S63845 for 4 days followed by CCK-8 assay to assess cell viability. Data are mean ± SD. ****, $P < 0.0001$. ***E***. HEY and OVCAR8 cells were first lentivirally transduced with BIRC5 for 1 day and further transduced with control,

FAP shRNA or REL shRNA for additional 4 days. Cell viability was assessed by CCK-8 assay. Data are mean ± SD. ****, $P < 0.0001$.

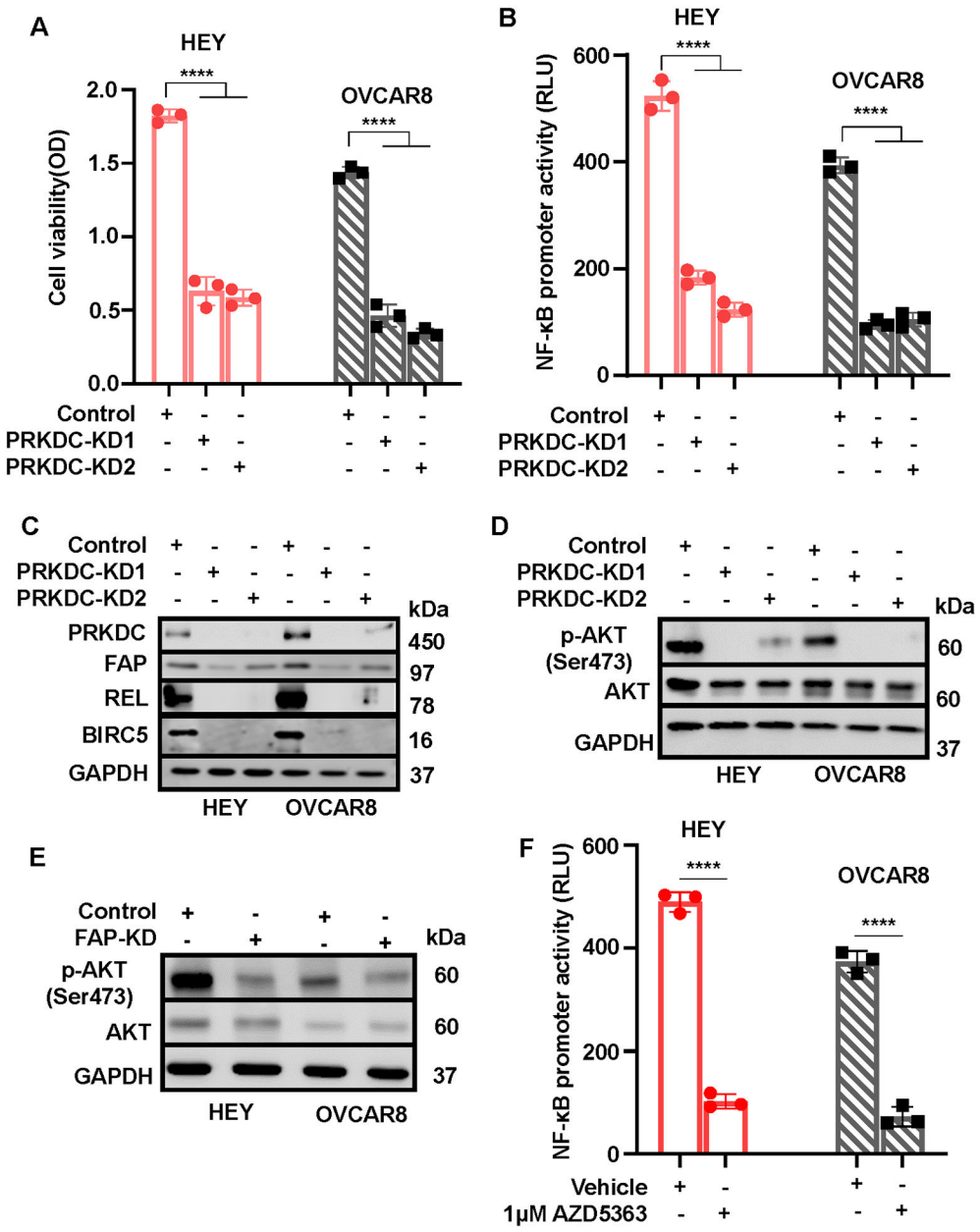

Figure 5. PRKDC is critically involved in NF-κB activation in ovarian cancer cells

A. HEY and OVCAR8 cells were lentivirally transduced with control or PRKDC shRNA for 4 days followed by CCK-8 assay to assess cell viability. Data are mean ± SD. ****, $P < 0.0001$.***B***. HEY and OVCAR8 cells were lentivirally transduced with control or PRKDC shRNA for 2 days and then transfected with NF-κB promoter reporter construct for another day followed by measuring luciferase activity. Data are mean ± SD. ****, $P < 0.0001$. ***C***. HEY and OVCAR8 cells were lentivirally transduced with control or PRKDC shRNA for 3 days and then lysed for western blotting to detect PRKDC, FAP, REL, BIRC5 and GAPDH with the respective antibodies. ***D***. Western blot analysis to detect phosphor-AKT (Ser473), AKT and GAPDH in HEY and OVCAR8 cells transduced with control or PRKDC shRNA. ***E***. Western blot analysis to detect phosphor-AKT (Ser473), AKT and GAPDH in HEY and

OVCAR8 cells transduced with control or FAP shRNA. ***F***. HEY and OVCAR8 cells were treated with vehicle (DMSO) or 1μM AZD5363 for 2 days and then subjected to CCK-8 assay to assess cell viability. Data are means ± SD. ****, $P < 0.0001$.

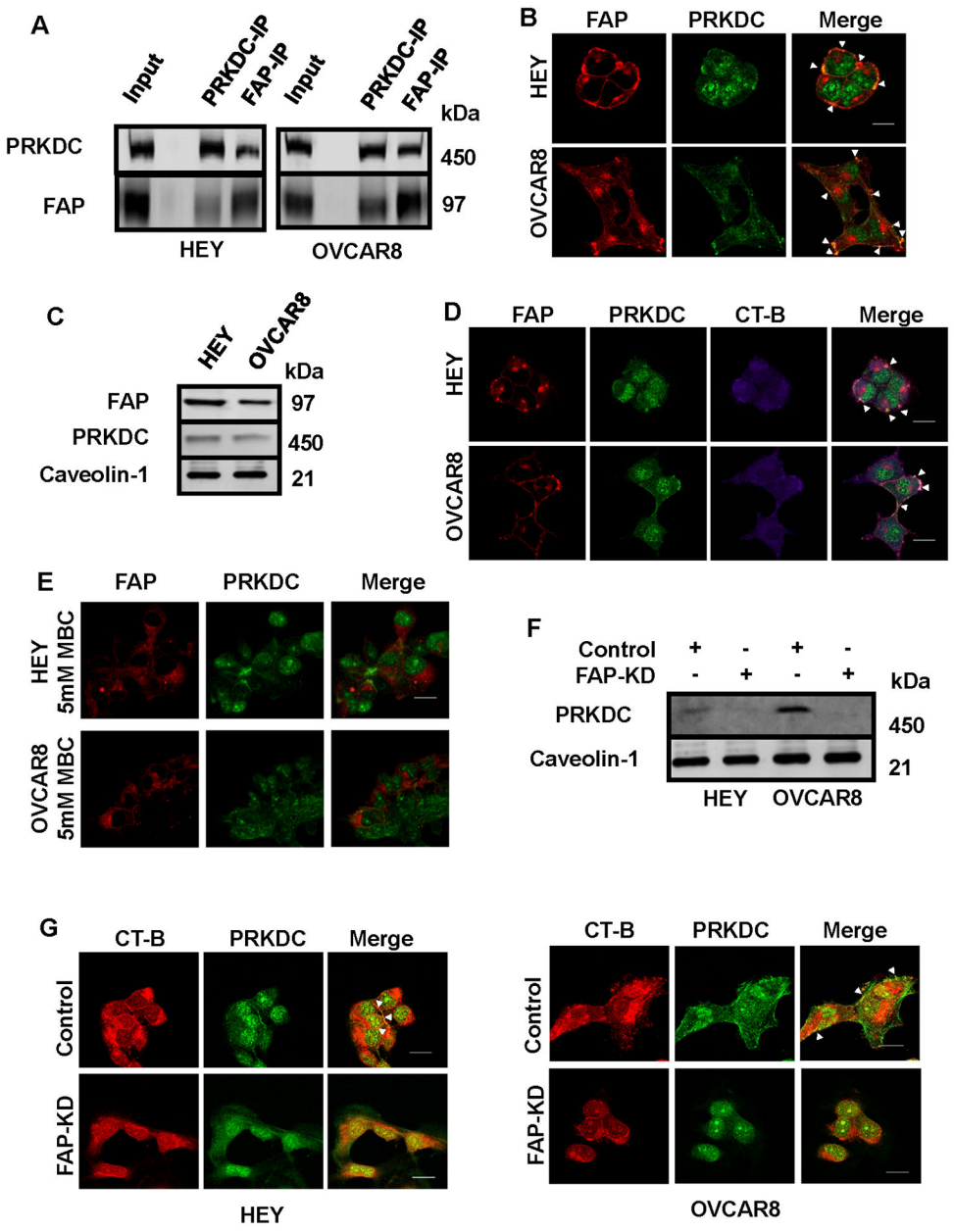

Figure 6. FAP-PRKDC interaction occurs in lipid rafts of ovarian cancer cells

A. HEY and OVCAR8 cells were immunoprecipitated with either anti-PRKDC or anti-FAP antibody and the immunoprecipitates were subjected to western blotting to detect FAP or PRKDC respectively. All blots derived from the same experiment and were processed in parallel. ***B***. HEY and OVCAR8 cells were subjected to immunofluorescence staining to detect FAP and PRKDC. Data are the representative of six independent experiments. ***C***. Lipid rafts were isolated from HEY and OVCAR8 cells and subjected to western blotting to detect PRKDC, FAP and caveolin-1 with the respective antibodies. ***D***. HEY and OVCAR8 cells were fixed and then stained for FAP and PRKDC with the respective antibodies. Labeled Cholera toxin subunit was also included for lipid raft staining. Data are the representative of six independent experiments. ***E***. HEY and OVCAR8 cells were

treated with 5mM MBC for 1 h and then subjected to immunofluorescence staining to detect FAP and PRKDC. Data are the representative of six independent experiments. ***F***. HEY and OVCAR8 cells were lentivirally transduced with control or FAP shRNA for 3 days and then subjected to lipid raft isolation. Western blot analysis was performed with these isolates to detect PRKDC and caveolin-1. ***G.*** HEY and OVCAR8 cells were lentivirally transduced with control or FAP shRNA for 3 days and then subjected immunofluorescence staining to detect PRKDC and lipid rafts. Data are the representative of six independent experiments.

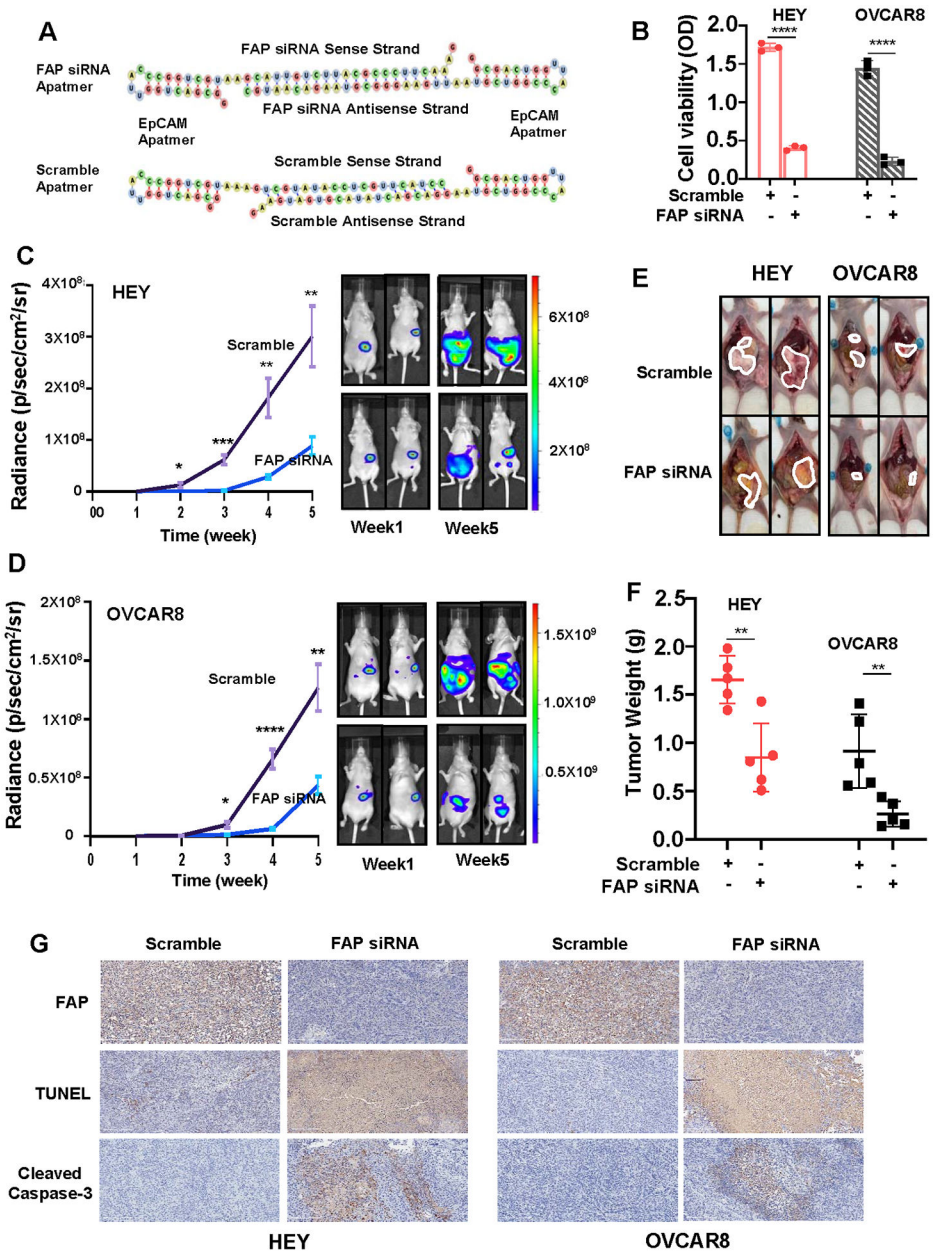

Figure 7. EpCAM aptamer-FAP siRNA chimera suppresses intraperitoneal xenograft development

A. Structure of EpCAM aptamer-FAP siRNA chimera. ***B***. CCK-8 assay to assess cell viability of HEY and OVCAR8 cells treated with control or EpCAP aptamer-FAP siRNA chimara. Data are means ± SD. ****, $P < 0.0001$. ***C, D***. Luciferase-expressing HEY (***C***) or OVCAR8 cells (***D***) (10^6 cells/mouse) were intraperitoneally injected into female athymic nude mice. One-week post tumor cell injection, mice were divided into two groups: one was treated with EpCAP aptamer-scramble chimera (control) and the other with EpCAM aptamer-FAP siRNA chimera. Intraperitoneal xenograft development was monitored weekly using the Xenogen IVIS-200 *In Vivo* bioluminescence imaging system. Left panel: xenograft development curve. Data are means ± SD. n = 5. *, $P < 0.05$; **, $P <$

0.01; ***, $P < 0.001$; ****, $P < 0.0001$. Right panel: Bioluminescent images of the xenograft tumors at the beginning (week 1) and end of treatment (week 5). Two representative mice from each group are shown. The image data are displayed in radiance (photons/sec/cm2/steradian). ***E***. Mice were sacrificed after 4 weeks of treatment and images were taken after dissection. Tumor implants are circled in white. ***F***. Tumor implants were collected and weighed. Data are means ± SD. **, $P < 0.01$. ***G***. Representative pictures of IHC staining on FAP, TUNEL and cleaved caspase-3 in tumor tissues derived from HEY and OVCAR8 cells.